JOURNAL OF MATERIALS SCIENCE **34** (1999) 4375–4383

Morphologies and physical properties of PA1010/HIPS/HIPS-g-MA ternary blends

GUANGXIN CHEN, JINGJIANG LIU*
Polymer Physics Laboratory, Changchun Institute of Applied Chemistry, Chinese Academy of Sciences, Changchun, 130022, People's Republic of China
E-mail: jjliu@ns.ciac.jl.cn

The effect of the content of a copolymer consisting of high impact polystyrene grafted with maleic anhydride (HIPS-g-MA) on morphological and mechanical properties of PA1010/HIPS blends has been studied. Blend morphologies were controlled by adding HIPS-g-MA during melt processing, thus the dispersion of the HIPS phase and interfacial adhesion between the domains and matrices in these blends were changed obviously. The weight fractions of HIPS-g-MA in the blends increased from 2.5 to 20, then much finer dispersions of discrete HIPS phase with average domain sizes decreased from 6.1 to 0.1 μm were obtained. It was found that a compatibilizer, a graft copolymer of HIPS-g-MA and PA1010 was synthesized *in situ* during the melt mixing of the blends. The mechanical properties of compatibilized blends were obviously better than those of uncompatibilized PA1010/HIPS blends. These behaviors could be attributed to the chemical interactions between the two components of PA1010 and HIPS-g-MA and good dispersion in PA1010/HIPS/HIPS-g-MA blends. Evidence of reactions in the blends was seen in the morphology and mechanical behaviour of the solid. The blend containing 5 wt% HIPS-g-MA component exhibited outstanding toughness.

1. Introduction

The need to broaden the performance spectrum of plastics has stimulated much interest in blending different types of polymers to obtain materials having a balanced combination of specific properties [1–3]. Most polymer pairs are thermodynamically immiscible, and, depending on composition, the viscosity, elasticity ratio of the components, the interfacial tension, and compounding conditions, and the complete different types of morphology, mechanical and rheological properties can be observed owing to the miscibility difference in these blends [4–6].

In order to make polymer alloys with high performance from an immiscible polymer mixture, a compatibilizer must be used to improve the interfacial adhesion and reduce the interfacial tension. Block or graft copolymers, generally known to be effective compatibilizers, can be preformed and added separately or be formed *in situ* by reaction between co-reactive functional groups in the polymer or additive during the melt blending process [7–9]. This copolymer, produced during the melt mixture, acts as a compatibilizer between two immiscible polymer components and it stays near the interface since the reaction between functional groups occurs easily near the interface [10–15]. Polymer alloys prepared by this technique have a very fine morphology and broader interface. Moreover, this fine morphology can persist under the very high shear stress found during the injection moulding process. In order to obtain this kind of alloy each polymer must have a specific reactive group, and both must react within 2–3 min if the extrusion or compounding time is considered. Reactive compatibilization, involving maleic anhydride block or grafted polyolefins, either used as a toughening agent for polyamides or as a compatibilizer for the polyamide/olefine blends, are probably among the most intensively investigated subjects reported in the literature. Other than maleic anhydride functional group, copolymers containing carboxylic acid, sulfonic acid, oxazoline and epoxy functional groups have also been employed.

In recent years, many blending systems, such as PA6/PS [16], PA6/ABS [17], PA6/PP [18], PA1010/PP [19], PA6/PE [20], PBT/HIPS [21], PBT/PS [22] and PET/ABS [23] were studied. However, rare research work has been carried out on the blend of HIPS and PA1010. In general, this blend system has important significance both in polymer science and in commercial application. As is well known, HIPS is a commercial product in large use. However, HIPS liners could meet problems in terms of the environment friendly blowing agents, HCFC-141b, from rigid polyurethane foam used for the insulation of domestic refrigerators and freezers. It was considered that the most convenient and cost effective solution would be to improve the HCFC-141b resistance of current HIPS materials through modification of the chemical composition, morphology and additives whilst another way would be to laminate with

* Author to whom all correspondence should be addressed.

a barrier layer on the foam contact surface. Polyamides have excellent solvent resistance and they exhibit superior barrier performance. A blend of PA1010 with HIPS is the best one in the Nylon family. Its cost is lower compared with PA11 and PA12 and the processing temperature of PA1010 matches that of HIPS better than is the case with PA6 and PA66. HIPS may undergo decomposition during blending it with PA6 or PA66 because their melting temperatures are over 250 °C. The compatibilized blends of HIPS and PA1010 have been used to manufacture the liners of refrigerators and freezers with HCFC-141b blowing agent successfully in China. From the scientific point of view, it is necessary to highlight the relationship among the miscibility, the effect of compatibilizer, morphology and mechanical properties of the blends of HIPS and PA1010. This is the main purpose of the research work.

We are trying to correlate the extent of compatibilization with the particle size and matrix adhesion through morphological studies and to correlate this morphology with the mechanical properties of PA1010/HIPS/HIPS-g-MA ternary blends. In particular PA1010 rich blends were investigated and optimum concentration of the compatibilizer for the improved performance of the blends is determined.

2. Experimental

2.1. Materials

HIPS employed in this study was a commercial grade (492-J) manufactured by Yanshan Petrochemical co. Beijing, China. 7% of polybutadiene is utilized during the polymerization of HIPS. Its MFR is 2.6 g/10 min. PA1010 was supplied from Jilin Shijinggou Union Chemical Co., China. Its relative viscosity is 2.1 and melting flow rate is 10 g/10 min.

2.2. Preparation of compatibilizer and blends

HIPS-g-MA was prepared by melt mixing initiated by dicumyl peroxide (DCP) in a Brabender mixing chamber. The mixing temperature is controlled at 180 °C. The content of MA in HIPS-g-MA used in this work was 4.7 wt %. The grafting degrees were determined by the chemical titration method.

PA1010 was dried for 24 h at 90 °C before melt blending. Ternary PA1010/HIPS/HIPS-g-MA blends were prepared by melt-mixed using a Brabender twin-screw extruder operating at a rotation speed of 20 rpm and mixing temperature designated as 210–235 °C.

2.3. Morphological observation

The morphology of the blends was observed with a scanning electron microscope (SEM, Jeol JXA-840) at an accelerating voltage of 25 kV. The blend samples were fractured at liquid nitrogen temperature, and the cryogenically fractured samples etched for 2 h to increase the contrast.

Specimens for transmission electron microscopy (TEM) observation were obtained by using cryoultramicrotomy at liquid nitrogen temperature. Ultrathin sections were stained with osmium tetroxide to enhance the contrast for the microscopy observations. A Jeol 1200EX TEM operated at 200 kV, was used to examine the morphology of these blends.

2.4. Mechanical properties

Testing specimens for mechanical properties were prepared by using a JSWF17SA injector with a barrel temperature of 220–240 °C. Measurements of tensile properties of specimens were carried out on an Instron 1121 machine at room temperature with cross-head speed of 5 mm/min. Measurements of flexural modulus and strength were also performed with an Instron 1121 on the basis of ISO178-1975E. The Izod impact test was carried out on a JJ-20 Model instrumented impact tester (made by Changchun Institute of Applied Chemistry, Chinese Academy of Sciences, and the Intelligent Instrument and Apparatus Institute of Changchun). The span was 40 mm; the capacity, 20 J; and the striking velocity, 3.8 m/s. Five specimens of each blend were tested and average values were taken as experimental data.

3. Results and discussion

3.1. Morphologies

Fig.1 shows the SEM micrographs of the etched blends of PA1010/HIPS and PA1010/HIPS/HIPS-g-MA. The effect of the compatibilizer on the morphology of the ternary blends is demonstrated in these pictures. HIPS was poorly dispersed in PA1010 without a compatibilizer. The HIPS particle size ranged from 2 to 10 μm with an average of about 6 μm. Poor interfacial adhesion was evident from the large voids left on the fracture surface where the particles had separated from the matrix and the smooth surface of the exposed HIPS particles (Fig. 1a). For the compatibilized blends, the HIPS was dispersed in the PA matrix. The presence of 5% HIPS-g-MA clearly resulted in smaller domain size. An even larger reduction in the dimensions of the dispersed phase was observed when higher concentration of compatibilizer was used. Interfacial adhesion seemed to be improved with increasing content of the compatibilizer because some of the HIPS particles had adhered to the matrix material. Better dispersion and improved interfacial adhesion should be attributed to the formation of HIPS-g-MA/PA1010 copolymer by reaction of anhydride groups with the terminal amine groups of PA1010 during the melt mixing. A narrowing of the domain size distribution for the compatibilized ternary blends was observed. It also was the effect of chemical reaction at interface. Fig. 2 shows the plot of the average particle size with the amounts of HIPS-g-MA in the blends. In the scope of investigated compositions, the average HIPS domain size decreased with increasing compatibilizer concentration from 0 to 20%.

As the particle size of HIPS decreased with increase in the HIPS-g-MA content, the number of particles increased, but the total volume fraction of the dispersed phase should not decrease. Since the SEM samples in this work had been extracted in THF (good solvent for HIPS), HIPS in uncompatibilized blends was removed by the solvent. For the compatibilized blends, it was impossible to remove all the dispersed phase because of the copolymer formation between HIPS-g-MA

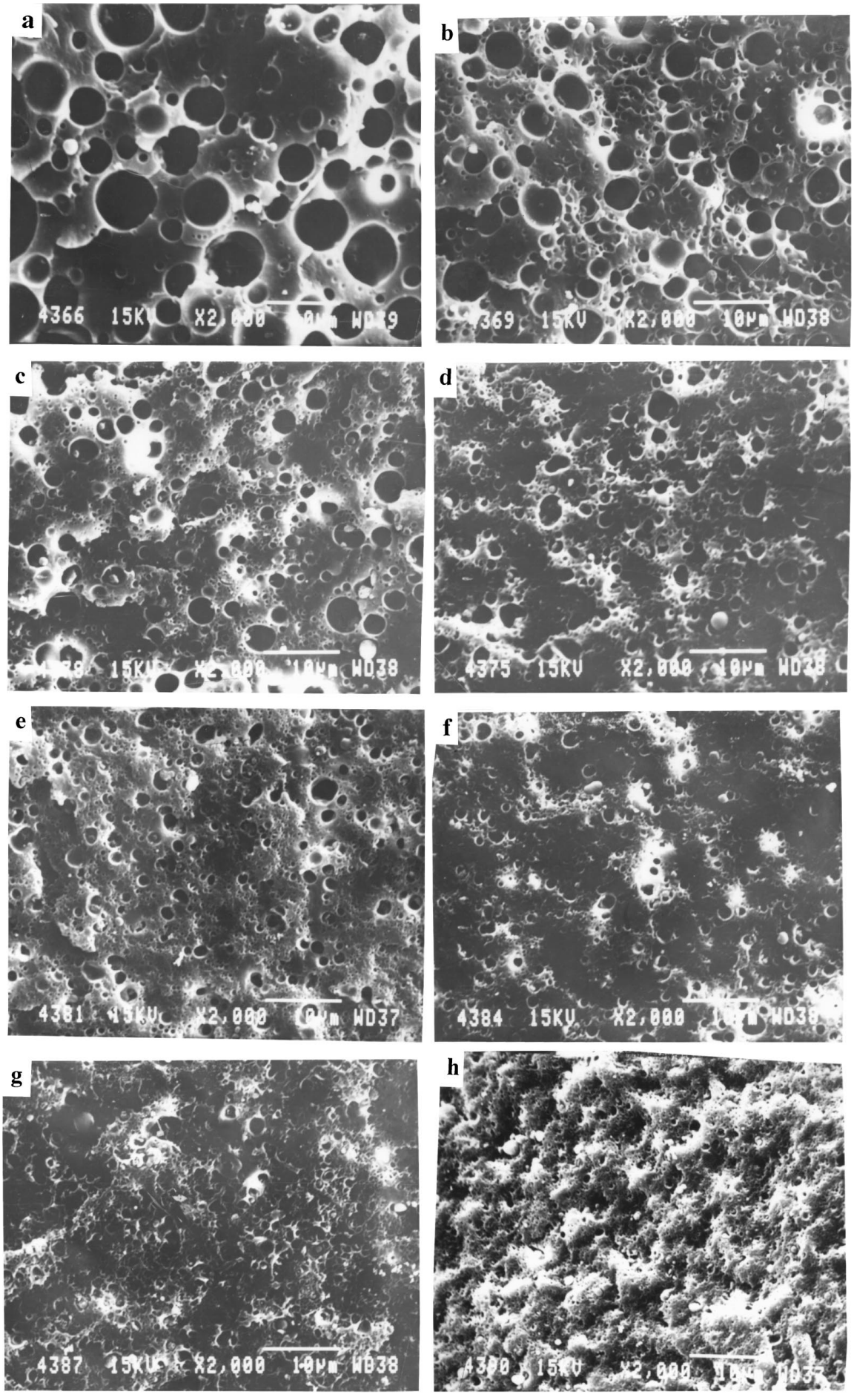

Figure 1 SEM micrographs of fractured surface of PA1010/HIPS/HIPS-g-MA blend: (a) 75/25/0 (b) 75/22.5/2.5 (c) 75/20/5 (d) 75/17.5/7.5 (e) 75/15/10 (f) 75/12.5/12.5 (g) 75/10/15 (h) 75/5/20.

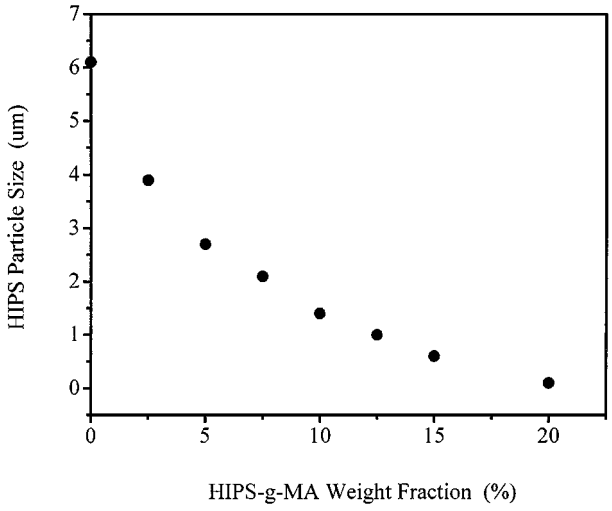

Figure 2 The plot of average particle size of the dispersed phase with the amount of HIPS-g-MA in the blends.

and PA1010 components. Therefore it is meaningful to measure the total area fraction of dispersed phase for understanding the mechanism of compatibilization. The measured area fractions of dispersed phase as a function of compatibilizer concentration is given in Fig. 3. It shows that the measured area fraction decreases as the HIPS-g-MA content in the blends increases, and it is also less than the calculated value of 0.25 based on composition. The reduction in the measured area fraction of the dispersed phase could be caused by the chemical reaction at the phase interface in the reactive extrusion, some of HIPS-g-MA has been reacted with PA1010 to form HIPS-g-PA1010 copolymer.

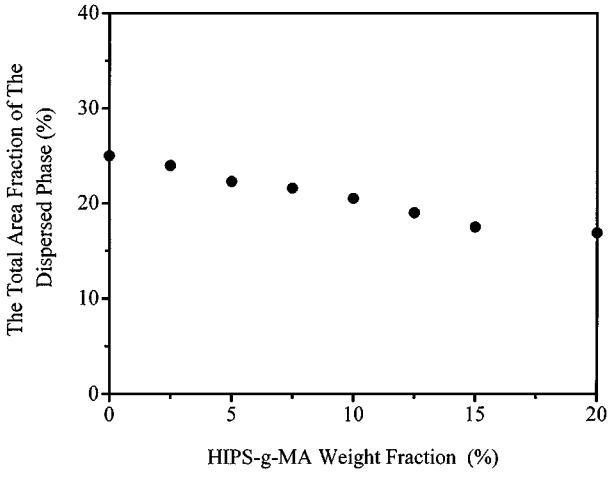

Figure 3 The total area fraction of the dispersed phase as a function of HIPS-g-MA concentration.

In order to identify the chemical reaction which occurred, we examined and discussed the morphology of ternary blends of PA1010/HIPS/HIPS-g-MA with an emphasis on the sequence of blending (Fig. 4). Fig. 4a shows an SEM micrograph of a (PA1010 + HIPS-g-MA)/HIPS blend, and Fig. 4b shows an SEM micrograph of a PA1010/(HIPS + HIPS-g-MA) blend. However, no obvious changes can be observed in the morphologies of the blends comparing with Fig. 4a and b. This probably comes from the strongly reactive ability between HIPS-g-MA and PA1010 and the graft copolymer of HIPS-g-PA1010 with effectual compatibilizied ability can be performed easily during the melt mixing process. As mentioned above, blends of PA1010 with HIPS-g-MA are subject to a chemical reaction during the melt mixing, which increases the interface adhesion and decreases the domain size. From the change of morphology shown in Fig. 4, we can also indicate that the material of HIPS-g-MA was an effectual compatibilizer on the system of PA1010/HIPS blends. Interfacial tension, the shear rate of mixing and the viscosity ratio of the blending components are key parameters governing the degree of dispersion [5]. When the shear rate of mixing and the viscosity ratio of the blended polymers are constant, the interfacial tension of the blend plays an important role in reducing the domain size. Therefore, better dispersion and the improved interfacial adhesion should be attributed to formation of the grafting copolymer at the interface between PA1010 and HIPS via reaction of MA in HIPS-g-MA with the terminal amine groups of PA1010 during the melt extrusion.

However, the SEM technique does not make it possible to distinguish the finer morphological features, in particular, the character of HIPS dispersion in blends with the graft copolymer, HIPS-g-MA. Majumdar *et al.* examined the morphologies of Nylon6/ABS blend compatibilized with SMA25 by TEM utilizing

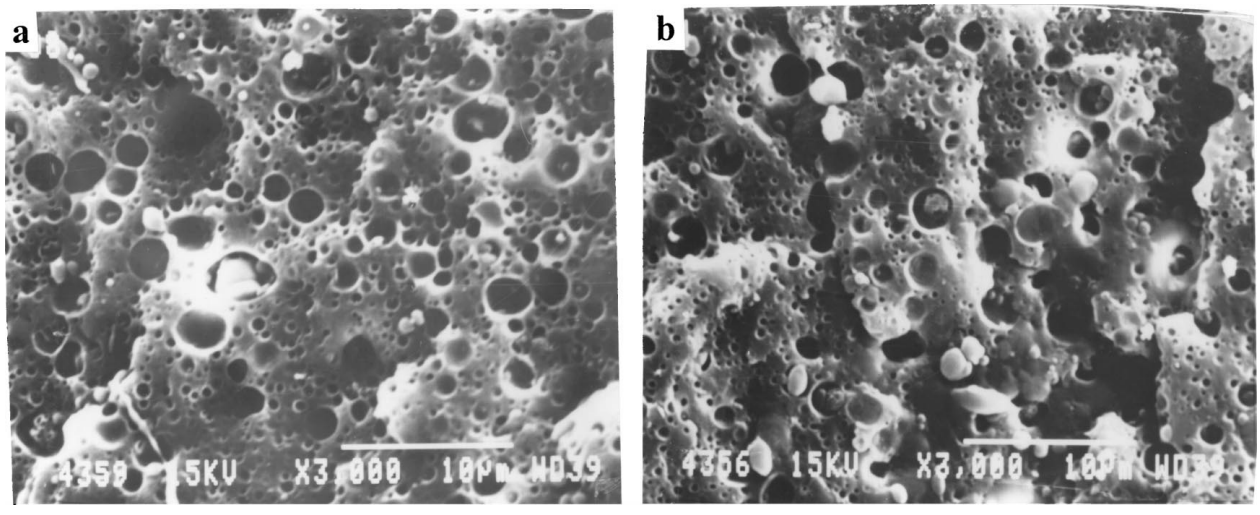

Figure 4 SEM micrographs of fractured surface of blends (a) (HIPS + HIPS-g-MA)/PA1010: 20 + 5/75 (b) (PA1010 + HIPS-g-MA)/HIPS: 75 + 5/20.

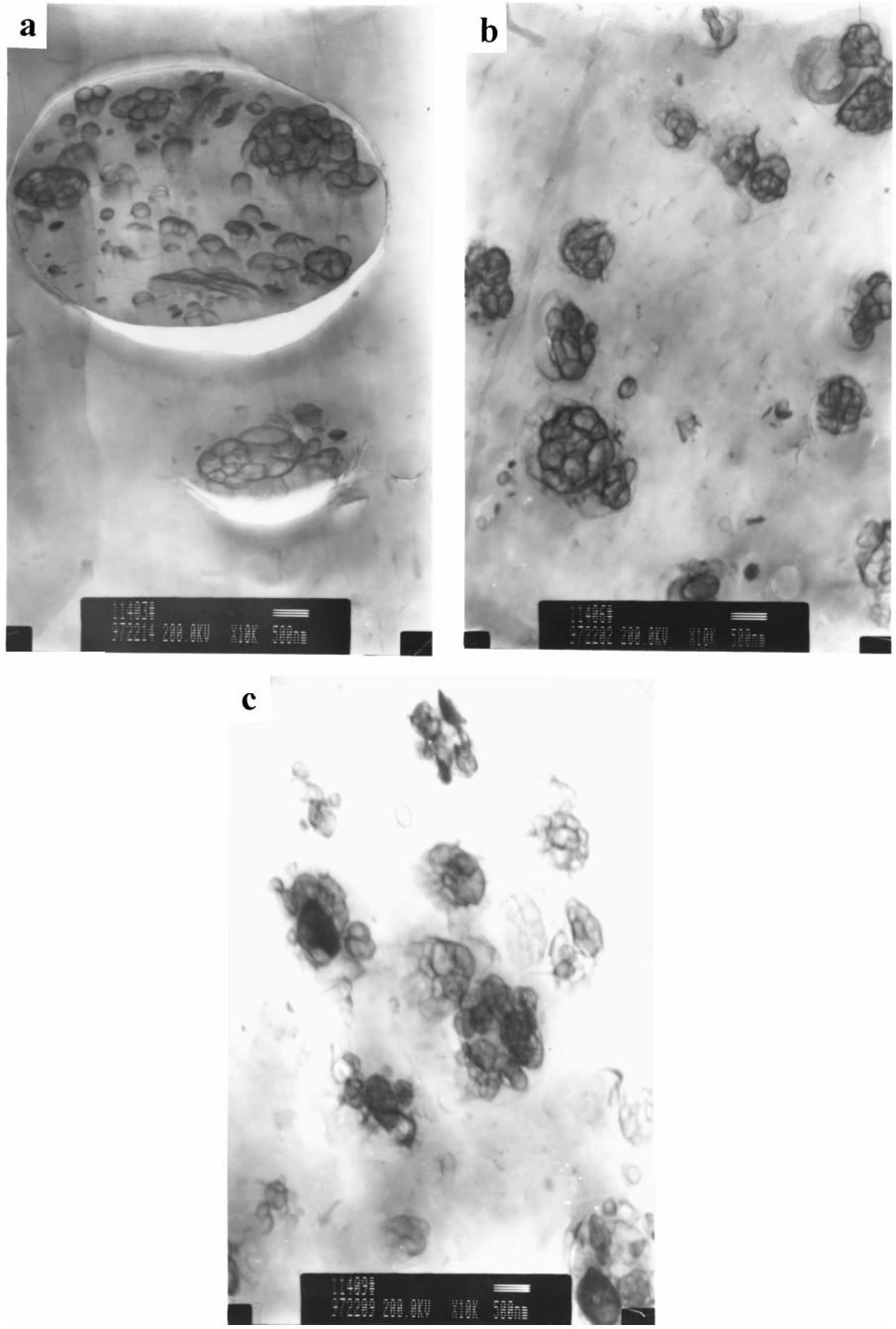

Figure 5 TEM micrographs for 75% PA1010 blends containing different xontents of HIPS-g-MA: (a) 0% (b) 5% (c) 10%. The samples were stained with O_sO_4.

several different staining techniques [24]. In order to examine the morphology features of compatibilized blends of PA1010/HIPS, the ultrathin sections of the blends were studied by using TEM. As expected, the TEM micrograph for the HIPS sample showed the complex cellular structure. The domain size has a broad distribution. Now, the morphologies of PA1010/HIPS blends compatibilized with HIPS-g-MA are examined by TEM. Fig. 5 shows micrographs of the series of blends containing 75% PA1010 with varying amounts of HIPS-g-MA. For the blends without any HIPS-g-MA copolymer, the cellular structure, rubber particles of the HIPS, exits in certain regions and the biggest diameter is about 10 μm. Comparing with the SEM micrograph, we can confirm that the regions are HIPS phases. The cellular structure, rubber particles of the HIPS, are entirely absent from other regions which must consist primarily of PA1010 (Fig. 5a). For the uncompatibilized blends, sharp boundaries and clear gaps between HIPS dispersed phase and PA1010 matrix were observed. The biggest domain size is about 10 μm in diameter. In these domains, the continuous phase consists of polystyrene while the cellular structure shown in HIPS was observed in the 75PA1010/25HIPS blend as the secondary dispersed phase. The domain size and its distribution are similar to that in HIPS. These results show that the cellular structure features and the morphological characteristic in HIPS are not broken and they are kept in the PA1010/HIPS blends totally. The worse miscibility between PA1010 and HIPS can be conducted from these observations. O_sO_4 staining techniques reveals the features and the distribution of polybutadiene chains in the domains. As well known, polybutadiene consists of the matrix in the cellar structure. They should be assigned

as the third phase morphology in PA1010/HIPS blends. For the compatibilized blends, the morphologies shown in Fig. 5b and c reveal that the sharp boundaries and clear gaps between the dispersed phase and the matrix have disappeared. Due to the interfacial reaction between PA1010 and HIPS-g-MA, the interfacial situation between PA1010 and HIPS is absolutely changed. Namely, the interface between PA1010 and HIPS is diffused and no clear layer of PS, as could be seen in the blend of PA1010/HIPS, can be identified. The site of the reaction on HIPS is the polybutadiene segment; hence, the PB chains should face toward the PA1010 matrix through the reaction. It means that the molecular architecture will affect the morphology of the blends and that the compatibilizer located at the interface broadens the interfacial region and that the molecular chains of HIPS-MA-PA1010 copolymer have penetrated into the adjacent phases of PA1010 and HIPS. In fact, the secondary dispersed phase identified clear in the uncompatibilized PA1010/HIPS blend can hardly be observed in the compatibilized blends. However, the third phase features still are maintained. After we examine the morphological features of the third dispersed phase carefully, the different characteristics among the compatibilized and uncompatibilized samples were confirmed. First, the regular spherical cellular structure shown in the uncompatibilized blends was detracted in the compatibilized blends. Secondary, the domains with cellular structure were distributed in the whole TEM images for compatibilized blends, on the contrary, they are concentrated in the PS domains in the uncompatibilized blend, i.e. a relatively high number of the third order of domains are visible in some regions while almost no domains are seen in other regions.

3.2. Izod impact properties

The incorporation of HIPS-g-MA in PA1010/HIPS blends results in a considerable increase in notched Izod impact strength over that of uncompatibilized blends of PA1010/HIPS (Table I). SEM micrographs of Izod fracture surfaces of PA1010/HIPS binary and PA1010/HIPS/HIPS-g-MA ternary blends are reported in Fig. 6. We found that the fracture surface of noncompatibilized blend is relatively smooth with

TABLE I Izod impact strength of the ternary blends

PA1010/HIPS/HIPS-g-MA	σ (MPa)
100/0/0	19.1
75/25/0	17.7
75/22.5/2.5	19.5
75/20/5	45.8
75/17.5/7.5	22.2
75/15/10	20.7
75/12.5/12.5	20.2
75/10/15	18.8
0/100/0	66.3

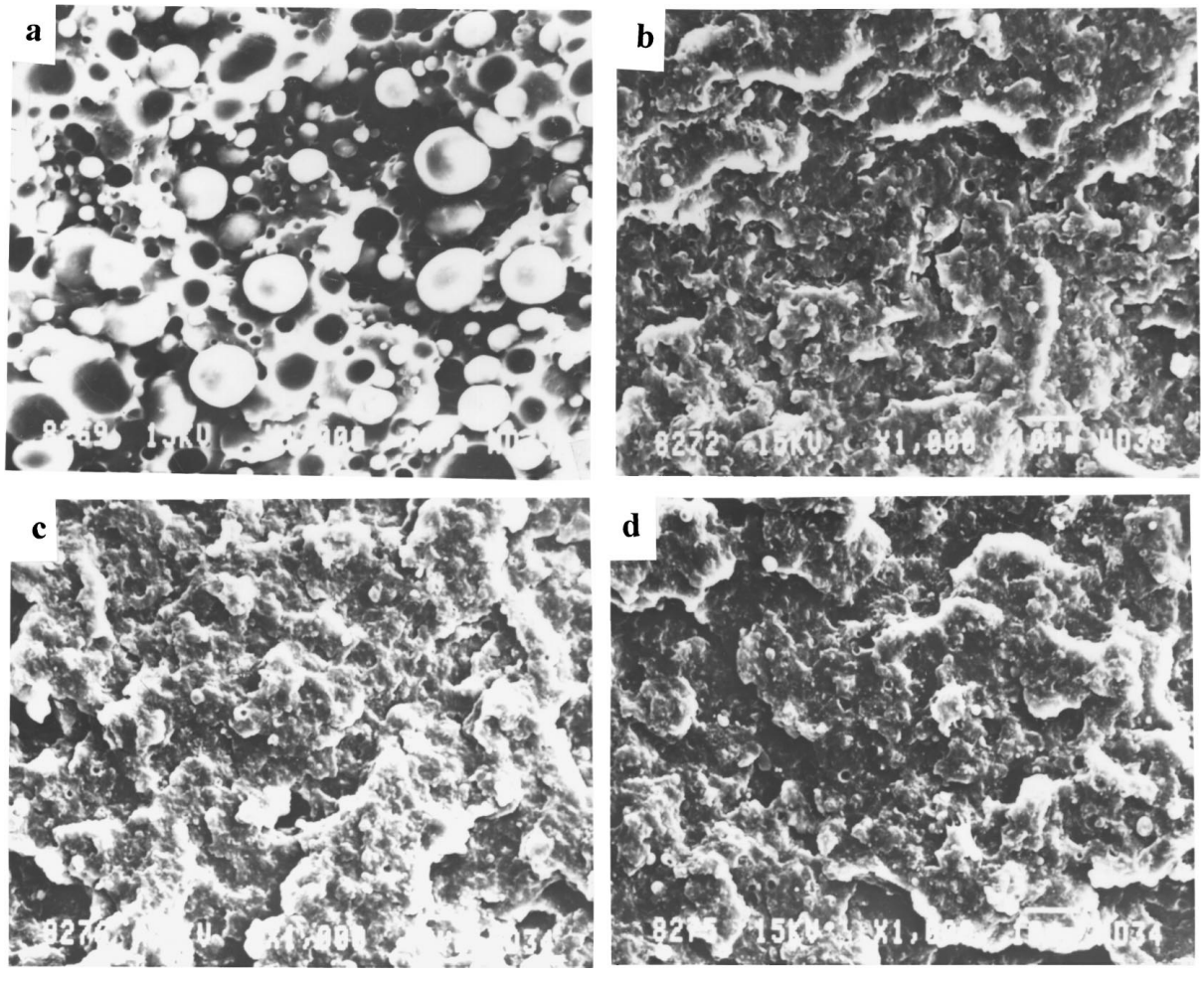

Figure 6 SEM micrographs of the Izod impact fracture surfaces containing (a) 0% (b) 5% (c) 10% (d) 15% HIPS-g-MA.

many spherical holes, which were exposed HIPS particles. When HIPS-g-MA was added, no HIPS particles are visible on the fracture surface. These behaviors should be attributed to the augmentation of adhesion between PA1010 and HIPS-g-MA components.

Interestingly, there appears to be an optimum level at about 5% HIPS-g-MA component in ternary blends. To characterize the toughness of the materials, the impact strength is a more convenient factor compared with the classical critical stress intensity factor (K_{IC}), which requires testing of very thick specimens for materials having low yield strength and high toughness, such as rubber toughened blends, in order to satisfy the small scale yield criterion [25]. Such thick specimens cannot be formed easily by injection moulding, which is a preferred method for fabricating plastic parts. For these reasons, the J-contour integral method has been recently regarded as more appropriate for such polymeric materials and has the benefit of not requiring exceedingly thick specimens [25]. A technique recently proposed by Vu-Khanh [26] offers an approach for characterizing fracture that is a useful compromise between rigorous fracture mechanics methodology and the simplicity of Izod or Charpy measurements. In this method, the energy required to fracture a specimen, U, with a ligament area, A, is measured by a standard or instrumented impact tester. It has the advantage of high test speeds corresponding to impact conditions as opposed to essentially static loading conditions usually employed in J_{IC} measurements. The analysis of these types of data as proposed by Vu-Khanh, yields a fracture energy at initiation, G_i, and a measure of the additional energy associated with propagating the fracture, or tearing modulus, T_a, Vu-Khanh has claimed that the fracture energy at initiation, G_i, is equivalent to the critical J-integral for fracture, J_{IC}. Mai [27] pointed out that the Vu-Khanh approach is equivalent to the essential work analysis proposed by Mai and coworkers and Hodgkinson and Williams [28–31] have questioned equating G_i to J_{IC}. Regardless of the interpretation used, this approach provides considerable useful information about the fracture process that goes well beyond the Izod or Charpy tests.

We investigated the G_i of blends, which reflected the toughness of materials. The plot of G_i vs. the content of HIPS-g-MA components in these blends is shown in Fig. 7 and the optimum level at about 5% HIPS-g-MA components was observed (Fig. 7). As shown in Fig. 7, the initial increase, of course, reflects the benefits of coupling the phases and the attendant morphology changes. The decline may reflect a loss in optimum morphology, embrittlement by excessive reaction, and possibly other causes. High HIPS-g-MA levels would embrittle the dispersed phase HIPS/HIPS-g-MA owing to the very brittle nature of HIPS-g-MA materials. However, at these relatively low levels, we believe that this is not the sole issue. Another factor is the relative stoichiometry of functional groups. For the ternary blends, the dispersed phase must contain enough HIPS-g-MA to have exactly as many MA units as there are PA1010 amine end-groups, assuming this is the only reactive site in the PA. Of course, full reaction of the

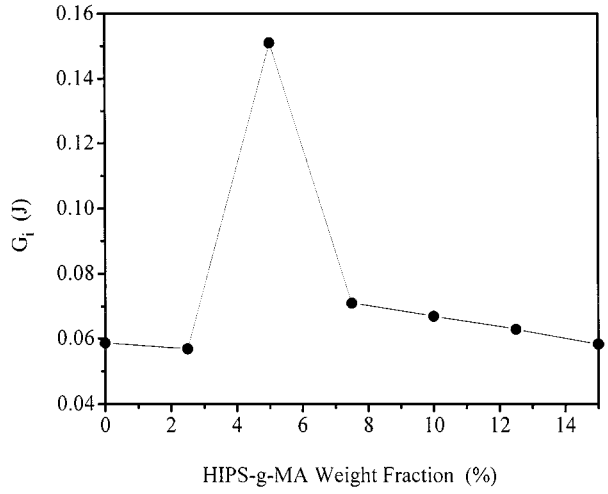

Figure 7 The plot of G_i with the amount of HIPS-g-MA in the blends.

HIPS-g-MA molecule would result in an extreme level of grafting per molecule. It is hard to imagine that this would be well suited for an interfacial role.

3.3. Tensile and flexural properties

Load-elongation curves for binary blends of PA1010/HIPS and ternary blends of PA1010/HIPS/HIPS-g-MA are shown in Fig. 8. It is seen that the uncompatibilized blends show no necking behavior, whereas all other blends show necking, indicating an increase in ductility. The tensile and flexural properties are reported in Table II and Fig. 9 shows the effect of compatibilizer on the tensile strength of PA1010/HIPS blends. It is observed that the tensile strength of all the blends compatibilized with HIPS-g-MA copolymer is higher than that of the corresponding binary PA1010/HIPS blend and the tensile strength of PA1010/HIPS blends goes on increasing with the addition of 2.5, 5, 7.5 and 10 wt % HIPS-g-MA compatibilizer, owing to improved homogeneity and decreased particle size. However, blends containing 12.5 wt % HIPS-g-MA component show a lower tensile strength than that of the blends containing 5 and 10 wt % HIPS-g-MA components. Tang and Huang [32] discuss this effect in terms of

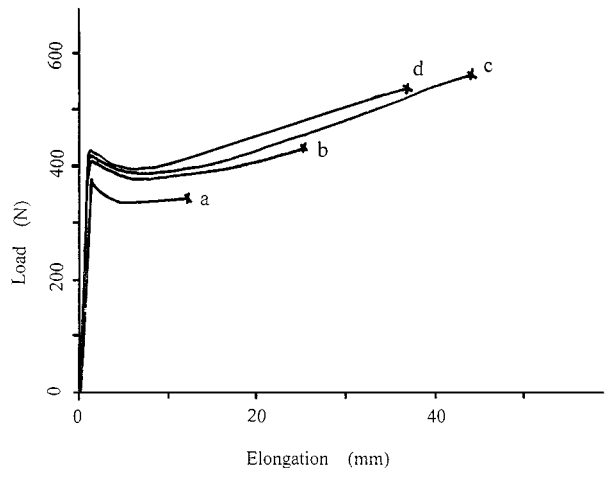

Figure 8 Load-elongation curves for PA1010/HIPS/HIPS-g-MA blend: (a) 75/25/0 (b) 75/20/5 (c) 75/15/10 (d) 75/10/15.

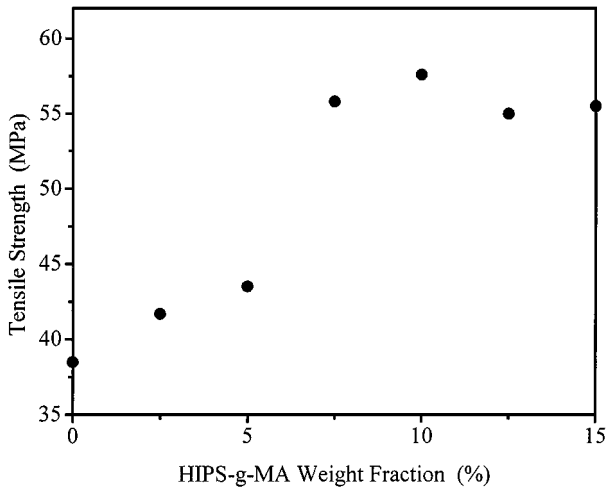

Figure 9 Tensile strength as a function of HIPS-g-MA weight percent for PA1010/HIPS/HIPS-g-MA blend.

effective concentration of compatibilizer. Up to the saturation level of the compatibilizer, molecules exist in the interfacial area between the dispersed phase and the matrix. But above this, only a part of it enters the interfacial area of the blend, influencing compatibilization. Hence, the actual amount of the compatibilizer used for improving the miscibility of the blend components is less than the quantity added. And the excess quantity only leads to its less effective participation as a compatibilizer, decreasing the homogeneity. This results in the requirement of optimum concentration of compatibilizer for each system.

TABLE II Tensile Strength σ_b, Elongation at Break ε_b, Energy E, Young's Modulus E_y, Flexural Strength σ_f and Flexural Modulus E_f of Ternary Blends

PA1010/HIPS/ HIPS-g-MA	σ_b (MPa)	ε_b (%)	E (J)	E_y (MPa)	σ_f (MPa)	E_f (MPa)
100/0/0	61	276.6	24.7	875.5	53.4	946.9
75/25/0	38.5	59.1	3.4	1078.5	56.3	1174.6
75/22.5/2.5	41.7	81.1	4.4	1028.6	59.8	1257.9
75/20/5	43.5	127.9	9.8	1036.2	56.8	1093.5
75/17.5/7.5	55.8	216.4	19.3	1044.9	57.1	1110.7
75/15/10	57.6	219.3	20.1	1024	62.6	1201.1
75/12.5/12.5	55	186.5	16.7	1013	63.9	1287.3
75/10/15	55.5	186	16.9	1093.2	64.3	1230.2
0/100/0	36.1	19.8	1.2	1280.1	51.9	1686.8

SEM images of the fracture surface are given in Fig. 10 for compatibilized and uncompatibilized blends of PA1010/HIPS. The distinct phase-separated domains are clearly seen for the uncompatibilized blends, while there are hardly any signs of a phase-separated morphology in the compatibilized blends of PA1010/HIPS/HIPS-g-PA1010 after a tensile test. Some other changes in the fracture surfaces were observed on the SEM micrographs as the amounts of compatibilizer increases. On the fracture of the PA1010/HIPS blends,

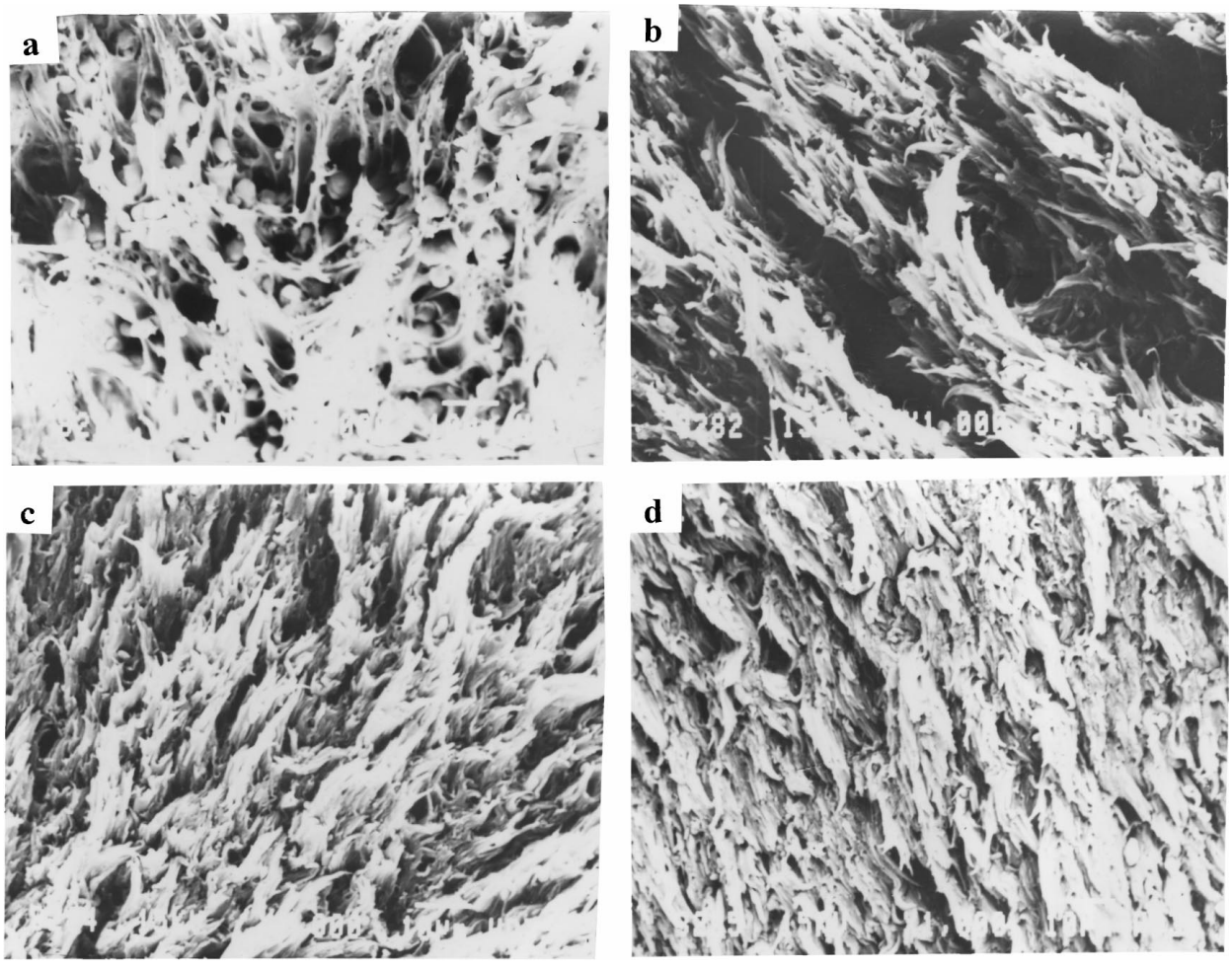

Figure 10 SEM micrographs of the tensile fracture surfaces containing (a) 0% (b) 5% (c) 10% (d) 15% HIPS-g-MA.

undeformed HIPS particles with smooth surfaces debonded from the surrounding PA, which was pulled out and fibrillated. This indicates that the interfacial adhesion is very poor between PA1010 and HIPS. However, in PA1010/HIPS/HIPS-g-MA blends, numerous thin ligaments connected HIPS particles to the deformed matrix and incorporated the particles into the fibrous PA1010 area. This evidences that adhesion between HIPS and PA1010 was good enough to prevent debonding during matrix drawing and indicated that the interfacial strength was higher than the fracture strength of the matrix. The ribbonlike features on the drawn ligaments were the result of recoil after they fractured. It was presumed that interfacial strength in the blends was determined primarily by interaction of the compatibilizer with PA, since adhesion to HIPS was provided by chemical linkages. The interaction of HIPS-g-MA with PA1010 was strong enough to sustain particle-matrix adhesion as the compatibilizer was drawn along with the PA. Interfacial agents generated *in situ* during the process of melt mixing through reaction between chemical functionalities available in the polymer chains have been reported in the literature. Both experimental observations and theoretical prediction indicate a reduction in the dispersed phase domain size. In addition, the presence of the compatibilizer at the interface broadens the interfacial region through penetration of the copolymer chains into the adjacent phase [33]. These factors mentioned above translated on the macroscale into higher fracture elongation for the blends.

4. Conclusion

The morphological studies show that the HIPS-g-MA behaves as an interfacial agent by improving the adhesion between HIPS particles and PA1010 matrix, significantly reducing the average dimensions of the HIPS dispersed phase from 6.1 to 0.1 μm. In addition, protruding objects and fibrous structure were observed. The blends containing 5 wt % HIPS-g-MA component exhibited outstanding toughness. These behaviors can be attributed to the homogeneous morphological dispersion of HIPS and the improved interfacial adhesion between matrix and dispersed phase owing to the chemical reaction between PA1010 and HIPS-g-MA.

References

1. L. M. ROBESON, *Polym. Eng. Sci.* **24** (1984) 587.
2. L. A. UTRACKI, *ibid.* **22** (1982) 1166.
3. M. XANTHOS, *ibid.* **28** (1988) 1392.
4. K. MIN, J. L. WHITE and J. F. FELLERS, *ibid.* **24** (1984) 1327.
5. S. WU, *ibid.* **27** (1987) 335.
6. B. D. FAVIS and J. WILLIS, *J. Polym. Sci., Polym. Phys. Ed.* **28** (1990) 2259.
7. M. XANTHOS and S. S. DAGLI, *Polym. Eng. Sci.* **31** (1991) 929.
8. D. CURTO, A. VALENZA and F. P. LA MANTIA, *J. Appl. Polym. Sci.* **39** (1990) 965.
9. P. VAN BALLEGOOIE and A. RUDIN, *Makromol. Chem.* **190** (1989) 3153.
10. I. PARK, J. W. BARLOW and D. R. PAUL, *J. Polym. Sci. Part B: Polym. Phys.* **30** (1992) 1021.
11. H. J. WON, D. P. CHAN and S. L. MOO, *Polymer* **37** (1996) 1709.
12. D. Y. CHANG, W. F. KUO and F. C. CHANG, *Polym. Networks Blends* **4** (1994) 157.
13. K. K. BYUNG and M. L. YOUNG, *Polymer* **34** (1993) 2075.
14. D. P. CHAN, H. J. WON and S. L. MOO, *ibid.* **37** (1996) 3055.
15. J. DUVALL, C. SELLITTI, V. TOPOLKARAEV, A. HILTNER, E. BAER and C. MYERS, *ibid.* **35** (1994) 3948.
16. H. J. WON, D. P. CHAN and S. L. MOO, *ibid.* **37** (1996) 1709.
17. Z. HORAK, Z. KRULIS, J. BALDRIAN and I. FORTELNY, *Polym. Networks Blends* **7** (1997) 43.
18. S. SATHE, G. S. S. RAO, K. V. RAO and S. DEVI, *Polym. Eng. Sci.* **36** (1996) 2443.
19. X. M. ZHANG, X. L. LI, D. M. WANG, Z. H. YIN and J. H. YIN, *J. Appl. Polym. Sci.* **64** (1997) 1489.
20. A. VALENZA, G. GEUSKENS and G. SPADARO, *Eur. Polym. J.* **33** (1997) 957.
21. D. Y. CHANG, W. F. KUO and F. C. CHANG, *Polym. Networks Blends* **4** (1994) 157.
22. J. K. KIM and H. LEE, *Polymer* **37** (1996) 305.
23. K. K. NIKOS, S. S. DIMITRIOS and K. K. JOANNIS, *ibid.* **37** (1996) 3387.
24. B. MAJUMDAR, J. KESKKULA and D. R. PAUL, *ibid.* **35** (1994) 3164.
25. J. G. WILLIAMS, "Fracture Mechanics of Polymers" (Ellis Horwood, Chichester, 1984).
26. T. VU-KHANH, *Polymer* **29** (1988) 1979.
27. Y. W. MAI, *Polym. Commun.* **30** (1989) 330.
28. Y. W. MAI and P. POWELL, *J. Polym. Sci., Part B: Polym. Phys.* **29** (1991)785.
29. Y. W. MAI and B. COTTERELL, *Int. J. Fracture* **32** (1986) 105.
30. Y. W. MAI, B. COTTERELL, R. HORLCK and G. VIGNA, *Polym. Eng. Sci* **27** (1987) 804.
31. J. HODGKINSON and J. G. WILLIAMS, *J. Mater. Sci.* **16** (1981) 50.
32. T. TANG and B. HUANG, *Polymer* **35** (1994) 281.
33. B. MAJUMDAR, D. R. PAUL and A. J. OSHINSKI, *ibid.* **38** (1997) 1787.

Received 13 January
and accepted 19 March 1999